VRIJE UNIVERSITEIT BRUSSEL

Vrije Universiteit Brussel
Faculteit Wetenschappen en
Bio-ingenieurswetenschappen
Departement Natuurkunde

Search for Dark Matter in the Monojet and Trackless Jets Final States with the CMS Detector at the LHC

Isabelle De Bruyn

Promotor
Prof. Dr. Steven Lowette

Proefschrift ingediend met het oog op het behalen van de
academische graad van Doctor in de Wetenschappen

September 2017

Acknowledgements

Table of Contents

1

Dark Matter Scenarios Beyond the Standard Model

In modern particle physics, the fundamental structure of matter at subatomic scales is described by the Standard Model [1, 2], which has already predicted many experimental results and is today considered among the most thoroughly tested scientific theories. The Higgs boson, the last missing piece which was predicted more than 50 years ago, was recently discovered at the Large Hadron Collider (LHC) in 2012 [3, 4], thus completing this elegant theory. Although it has survived many precision tests so far, the Standard Model only describes 5% of the matter and energy in the known universe and is unable to explain many unresolved questions and observations, such as the baryon asymmetry, dark matter and dark energy, the neutrino masses, the incorporation of gravity, and the hierarchy problem.

In this chapter, a brief description of the Standard Model is first given in Section 1.1, including its shortcomings. In Section 1.2, one of the missing pieces in the Standard Model, dark matter, is discussed. The observational evidence for dark matter, as well as possible models and detection mechanisms are detailed. Finally, in Section 1.3 one of the dark matter models considered in this thesis is described in detail.

1.1 The Standard Model of Particle Physics

The Standard Model of elementary particle physics has been developed during the second half of the 20th century, and reached its current formulation in the 1970's with the combination of the electromagnetic and weak interactions into the electroweak interaction [5–7], incorporating the Brout-Englert-Higgs (BEH) mechanism [8–10], and the addition of asymptotic freedom [11, 12] into the theory of the strong interaction. It is a quantum field theory which describes the fundamental particles and their interactions, incorporating three of the four fundamental forces. While this consistent framework describes the electromagnetic force and the weak and strong nuclear interactions, the fourth interaction, gravity, has not yet been included successfully.

1.1.1 Elementary particles and their interactions

All ordinary matter we see around us is built up from atoms, which consist of negatively charged electrons circulating around the positively charged atomic nucleus, formed by protons and neutrons, which in turn consist of up and down quarks. The electrons and up and down quarks are fundamental particles called fermions. Although all ordinary matter can be built from this so-called first generation of fermions, there are twelve fermions with different flavours in total, six quarks and six leptons, grouped in three

generations with increasing mass, as shown in Figure 1.1. The electrically neutral neutrinos interact only via the weak nuclear interaction, which complicates their observation, but they can be detected in dedicated experiments.

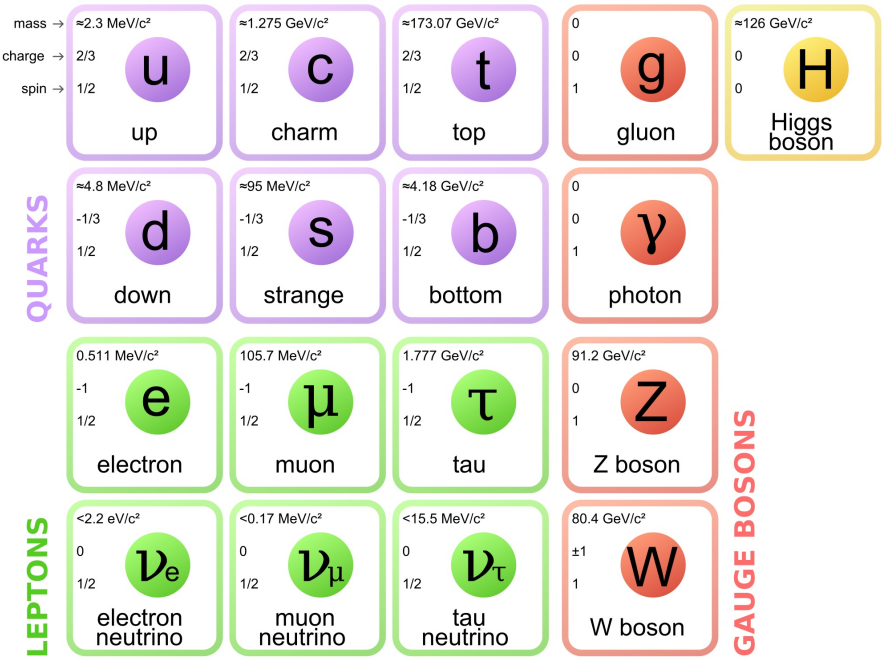

Figure 1.1: The particle content of the Standard Model, showing the fermions divided into 3 generations (columns) on the left and the bosons on the right. The electrical charges are expressed as multiples of the absolute value of the electron charge. Figure taken from [13].

A common characteristic of the fermions is their half-integer spin, in contrast to the integer spin of the force mediators, called bosons. Within the Standard Model, the mediation of the different fundamental interactions is represented by the exchange of these spin-1 gauge bosons, which are summarized in Figure 1.1. The massless photon mediates the most familiar force, the electromagnetic interaction, which is responsible for light, electromagnetic fields, and chemical reactions. The weak nuclear interaction is among other things used to describe the radioactive β decay, and is propagated by the neutral Z boson and and two charged massive W bosons. Lastly, the strong nuclear interaction is carried by massless gluons, keeping the protons and neutrons in the atomic nuclei and holding the quark constituents together. A resulting property of the quarks is that they hadronise, i.e. they cannot exist isolated, but form bound states via the strong interaction. These bound states are referred to as hadrons, and can be made up from three quarks or a quark and an antiquark, respectively called baryons and mesons.

Finally, it is also important to note that for every fermion (f) there exists an antifermion $(\bar{f})$, which differs only in electric charge and handedness of spin. When matter and antimatter come into contact they annihilate, generating energy which can be transformed into other particles.

1.1.2 The theoretical framework of the Standard Model

The Standard Model goes further than merely giving an exhaustive list of elementary particles, it has a supporting theoretical framework formulated as a relativistic quantum field theory. In a quantum field theory, every particle is represented by discrete excitations of a field $\psi(x)$, where x is the space-time coordinate. The interactions and kinematics of this particle are fully determined by the action S, which is defined as the integral of the Lagrangian $\mathcal{L}(\psi(x), \partial^\mu\psi(x))$ over the space-time coordinates:

$$S = \int \mathcal{L}(\psi(x), \partial^\mu\psi(x))d^4x. \tag{1.1}$$

The Lagrangian is a function of the field $\psi(x)$ and its first derivative $\partial^\mu\psi(x)$, where μ represents the index of the space-time coordinate. The physical behaviour of the particles is obtained by following the principle of least action $\delta S = 0$, minimizing the action.

In this framework based on the gauge invariance of the Lagrangian under the fundamental symmetries, the interactions between the fermions and bosons follow automatically. This can be illustrated with the following example for invariance under a general local gauge transformation.

As mentioned before, a fermion has a half integer spin and can thus be represented as a complex relativistic spin-1/2 field, called a Dirac spinor:

$$\mathcal{L}_{Dirac} = i\bar{\psi}\gamma^\mu\partial_\mu\psi - m\bar{\psi}\psi, \tag{1.2}$$

where γ^μ are the Dirac matrices, and the adjoint field $\bar{\psi} = \psi^\dagger\gamma^0$ is the field associated to the antifermion. The imposed local gauge invariance then requires the fermion fields, and the overall Lagrangian, to be invariant under so-called local phase transformations

$$\psi \to \psi' = U(x)\psi = e^{i\vec{\alpha}(x)\cdot\frac{\vec{\tau}}{2}}\psi \tag{1.3}$$

where $\vec{\alpha}(x)$ are the space-time dependent rotation parameters in the symmetry group represented by the Lie group generators $\vec{\tau}$. Since the derivative ∂_μ in (1.2) spoils the invariance of the Lagrangian under a local phase transformation, it is replaced with a covariant derivative

$$D_\mu = \partial_\mu - ig\frac{\vec{\tau}}{2}\vec{A}_\mu, \tag{1.4}$$

restoring the invariance. This however introduces new vector gauge fields A_μ, which interact with the fermion fields with a coupling strength g. As a result, the Dirac Lagrangian contains an additional term, which describes the interaction between the fermion fields mediated by the gauge fields A_μ, and (1.2) becomes

$$\mathcal{L}_{Dirac} = i\bar{\psi}\gamma^\mu\partial_\mu\psi - m\bar{\psi}\psi + g\bar{\psi}\gamma^\mu\psi\vec{A}_\mu\cdot\frac{\vec{\tau}}{2} \tag{1.5}$$

The matrix $U(x)$ which was introduced above, was defined as a general rotation matrix of the symmetry group $SU(N)$. In order to obtain the three fundamental interactions of the Standard Model, the described procedure can be simplified using the corresponding symmetry groups as mentioned below.

Electroweak theory
The electroweak interaction describes the electromagnetic and weak interactions, which appear very different at low energies but can be merged into a single electroweak force above the electroweak energy scale. This theory is described by requiring gauge invariance under the $SU(2)_L \otimes U(1)_Y$ symmetry group. This leads to 3 gauge fields W_μ^α introduced by the $SU(2)_L$ group, and one gauge field B_μ from the $U(1)_Y$ group. Two coupling constants are introduced, g_1 and g_2, for $U(1)_Y$ and $SU(2)_L$, respectively. The corresponding observable gauge bosons are the photon, the Z^0, and the $W^\pm$ bosons.

Quantum Chromodynamics (QCD)
The strong interaction is described by the theory of Quantum Chromodynamics and is represented by the symmetry group $SU(3)$. It describes the interaction between particles that carry a colour charge, which can be red, green, blue, or one of the three corresponding anticolours. There are eight gauge boson fields associated to this group, which are massless and known as gluons. An important aspect which is unique for this interaction is asymptotic freedom, which states that the strong coupling constant, denoted by α_s, goes to zero at high energies. Consequently, the strong force becomes stronger as the distance between the strongly interacting quarks and gluons increases. As a result, the quarks and gluons cannot exist independently and are not observed individually, but are instead confined in colour-neutral hadrons. This effect is called confinement.

At this point the resulting Lagrangian including the three fundamental forces does not contain any mass terms, and so it cannot explain the observed particle masses. Additional mass terms cannot simply

be added explicitly because they would break gauge invariance. Instead, a solution to this problem is found by introducing a complex scalar doublet ϕ with a non-zero vacuum expectation value (vev) v. This breaks the electroweak symmetry and is known as the Brout-Englert-Higgs (BEH) mechanism, postulated in 1964 [8–10]. The Lagrangian of the Higgs field is

$$\begin{aligned}\mathcal{L}_H &= (D^\mu\phi)^\dagger(D_\mu\phi) - V(\phi) \\ &= (D^\mu\phi)^\dagger(D_\mu\phi) - \frac{1}{2}\mu^2\phi^\dagger\phi + \frac{1}{4}\lambda^2(\phi^\dagger\phi)^2,\end{aligned} \tag{1.6}$$

where μ is a real constant representing a mass parameter and λ is a dimensionless parameter standing for the self-interaction strength. The potential V of the scalar doublet has an infinite set of minima or ground states, and by choosing a ground state and expanding the field around it, the electroweak symmetry is broken. As a result, three of the four original fields of the scalar doublet are absorbed by the massless vector fields of the weak interaction, giving mass to the W and Z bosons:

$$M_W = \frac{1}{2}vg_2 \qquad M_Z = \frac{1}{2}v\sqrt{g_1^2 + g_2^2}. \tag{1.7}$$

From the remaining field, the H boson arises, acquiring a mass $m_H = \sqrt{2\lambda v}$.

The introduction of mass terms for the fermions also follows from the BEH mechanism, which allows to insert the following gauge-invariant term in the Lagrangian:

$$\mathcal{L}_{Yukawa} = -Y_{ij}\bar{\psi}_{L,i}\phi\psi_{R,j} + h.c. \tag{1.8}$$

with the Y_{ij} Yukawa matrices. The L and R here denote left-handed and right-handed fermions. This handedness or chirality is defined as $\psi_L = \frac{1}{2}(1-\gamma_5)\psi$ for left-handed and $\psi_L = \frac{1}{2}(1+\gamma_5)\psi$ for right-handed fermions. The fermion masses then arise from the Yukawa interactions describing the couplings of the fermions with the Higgs field. For massive particles, a reference frame which overtakes the spinning particle can always be found, in which case the particle will seem to move backwards, flipping its helicity[1]. This is however not the case for massless particles, which travel at the speed of light. As only left-handed neutrinos and right-handed antineutrinos have been observed so far, the neutrinos are massless in the Standard Model.

1.1.3 Unanswered questions of the Standard Model

Although the Standard Model is an extremely successful theory, there are still many questions that remain unanswered, indicating that the Standard Model cannot be a complete theory of nature. A brief description of some of the main unsolved problems follows here.

Grand Unified Theory

As the weak and electromagnetic interactions were successfully unified into the electroweak one, the idea of representing the three forces of the Standard Model by a single one is envisaged and studied. While this Grand Unified Theory (GUT) could be a first step towards the incorporation of gravity in the Standard Model, it cannot be achieved with the current Standard Model and requires new physics at a very high energy scale.

Baryon asymmetry

This problem refers to the imbalance of matter and antimatter in the universe. While the Big Bang should have produced an equal amount of baryonic and antibaryonic matter, this is not measured in our observable universe. It is assumed that most of the primordial matter and antimatter annihilated, but an imbalance allowed a fraction of the matter to survive. Within the Standard Model, some asymmetry in the production of matter and antimatter could be explained by the CP-violation[2] of the weak interaction. However, the amount of CP-violation needed to explain the baryon asymmetry is ten times higher than is observed from Standard Model measurements.

[1] The helicity is defined as the sign of the projection of the spin vector onto the momentum vector of a particle, left is negative and right is positive.

[2] According to Charge Parity (CP) symmetry, the laws of physics should remain identical when converting a particle into its antiparticle and mirroring the space coordinates. However, measurements of e.g. kaon-antikaon mixing show that this symmetry is violated.

Hierarchy problem
The most important hierarchy problem concerns the question why the weak force is so much stronger than gravity. The measured vector boson masses suggest that the electroweak symmetry breaking should occur at an energy scale of $\mu^2 \sim (100 \text{ GeV})^2$, while the energy regime where gravity becomes comparable to the other forces, called the Planck scale, is of the order of $\Lambda_{Planck} \sim 10^{19}$ GeV. This question is related to the mystery as to why the Higgs boson mass is so much smaller than the Planck scale. The real physical Higgs boson mass is composed of its bare mass and quantum loop corrections. These corrections depend strongly on a cut-off scale, which would be the Planck scale if no additional physics on top of the Standard Model is present up to this scale. In order for the theoretical prediction to match the experimentally determined mass of 125 GeV, the bare mass would need to be tuned to cancel the huge quadratic radiative corrections. This would require a significant fine-tuning of more than 30 orders of magnitude, which is not desirable for any theory.

Neutrino masses
The Standard Model predicts that the neutrinos are massless weakly interacting particles, but observations by the Sudbury Neutrino Observatory [14] and Super-Kamiokande [15] collaborations showed the first clear evidence that the neutrinos oscillate from one flavour into another. This can only be explained if the neutrinos differ in mass, implying that they are not massless. As mentioned above, the Standard Model does not provide masses for the neutrinos and it should therefore be extended to explain this observation.

Dark matter and energy
This mystery arises from cosmological observations, which indicate that the known matter described by the Standard Model makes up only 5% of the matter and energy in the universe. The remaining matter, called dark matter, contributes another 27%, and will be discussed in more detail in Section 1.2. In the Standard Model, neutrinos contribute to the dark matter, but their relic density is by far not enough to account for all the dark matter. The last 68% has been labelled dark energy and is believed to be responsible for the acceleration of the observed expansion of the universe, but remains even more enigmatic as no explanation can be provided by the Standard Model.

1.2 Dark matter

One of the current open questions in particle physics that is not answered by the Standard Model is the existence of dark matter. Many astrophysical observations from gravitational effects (see for instance [16]) show there must be some additional matter in the universe, the so-called dark matter, next to the known matter. Despite this, its precise nature remains as of yet unknown. Countless theoretical models are being constructed in order to explain its origin, and on the experimental side dark matter is being looked for in many different ways, but no observation has been made so far.

1.2.1 Observational evidence

The first hints of dark matter were observed by F. Zwicky [17] in 1933 by studying the velocity dispersion of galaxies in the Coma cluster. The effect is not only observed for entire galaxies, but also for various luminous objects, such as stars or gas clouds, inside a galaxy. The rotation curves of galaxies have been well studied, and show clear evidence for the existence of dark matter. An example of a rotation curve is shown in Figure 1.2, exhibiting a flat behaviour of the rotational velocity at large distances, going even far beyond the edge of the visible disk. However, in Newtonian dynamics the circular velocity is expected to be

$$v(r) = \sqrt{\frac{GM(r)}{r}}, \tag{1.9}$$

where $M(r) = 4\pi \int \rho(r) r^2 dr$ with $\rho(r)$ the mass density profile. Assuming $M(r)$ to be constant, the circular velocity is expected to fall like $1/\sqrt{r}$ beyond the disk. Since the measurements show an approximately constant velocity but a dropping visible mass density, this implies the existence of a halo with

$M(r) \propto r$ and $\rho(r) \propto 1/r^2$. A universal density profile seems to be suggested by the rotation curves of both low and high surface luminosity galaxies, consisting of an exponential thin stellar disk and a spherical dark matter halo with a flat core of radius r_0 and density $\rho_0 = 4.5 \times 10^{-2} (r_0/\text{kpc})^{-2/3} \text{M}_\odot \text{pc}^{-3}$ [18][3].

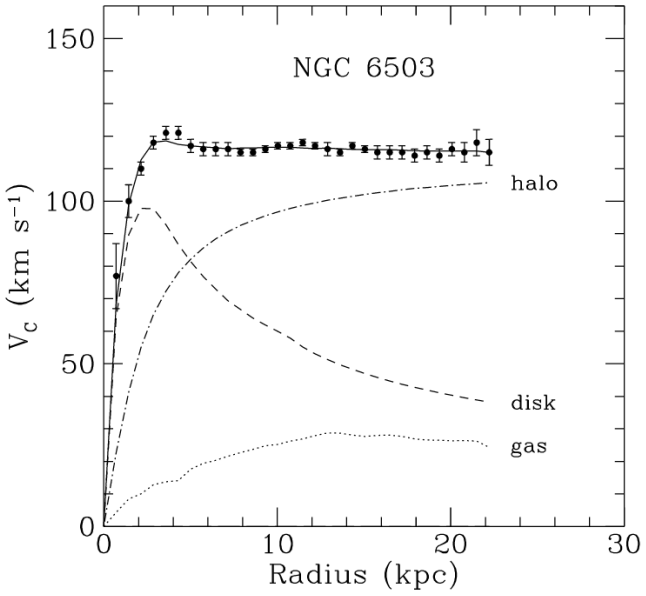

Figure 1.2: Rotation curve of NGC 6503. The dotted, dashed, and dash-dotted lines show the contributions of gas, disk, and dark matter, respectively. Figure taken from [19].

Another evidence for dark matter comes from the effect of gravitational lensing, allowing to determine the mass of an object regardless of the light it emits. When a distant star or quasar is aligned with a massive compact object, the bending of its light due to the gravitational field of the massive object can lead to multiple distorted, magnified, and brightened images, as illustrated in Figure 1.3. The distortion of the image can then be used to determine the potential well and thus the mass of the heavy object. Yet another way to determine the mass of a cluster of galaxies, next to gravitational lensing and the distribution of radial velocities, is by studying the profile of X-ray emission, tracing the distribution of the hot emitting gas in clusters. In general, these three methods are in reasonable agreement with each other.

Additionally, at a cosmological level, the analysis of the Cosmic Microwave Background (CMB) allows to determine the total amount of dark matter in the universe. The existence of this isotropic background radiation was already predicted in 1948, and unintentionally discovered by A. Penzias and R. Wilson in 1965 [21]. This relic radiation comes from the propagation of photons in the early universe, once they decoupled from matter. Before this, the photons were energetic enough to ionise hydrogen, creating a plasma of electrons and protons which were unable to combine into hydrogen. As the universe expanded and cooled down, the photons also cooled down enough to let the hydrogen atoms recombine, and the universe became transparent. The photons can then travel freely without scattering off the protons and electrons of the plasma, still carrying information from this surface of last scattering. The CMB is now known to be isotropic at the level of 10^{-5} and to follow the spectrum of a black body corresponding to a temperature of 2.726 K. However, small anisotropies in the CMB have first been observed by the COBE satellite [22] and more recently by WMAP [23] and Planck [24], as can be seen in Figure 1.4. These anisotropies correspond to small thermal variations, and are usually expanded as

$$\frac{\delta T}{T}(\theta, \phi) = \sum_{l=2}^{+\infty} \sum_{m=-l}^{+l} a_{lm} Y_{lm}(\theta, \phi), \tag{1.10}$$

[3] $\text{M}_\odot$ denotes a solar mass, 2×10^{30} kg.

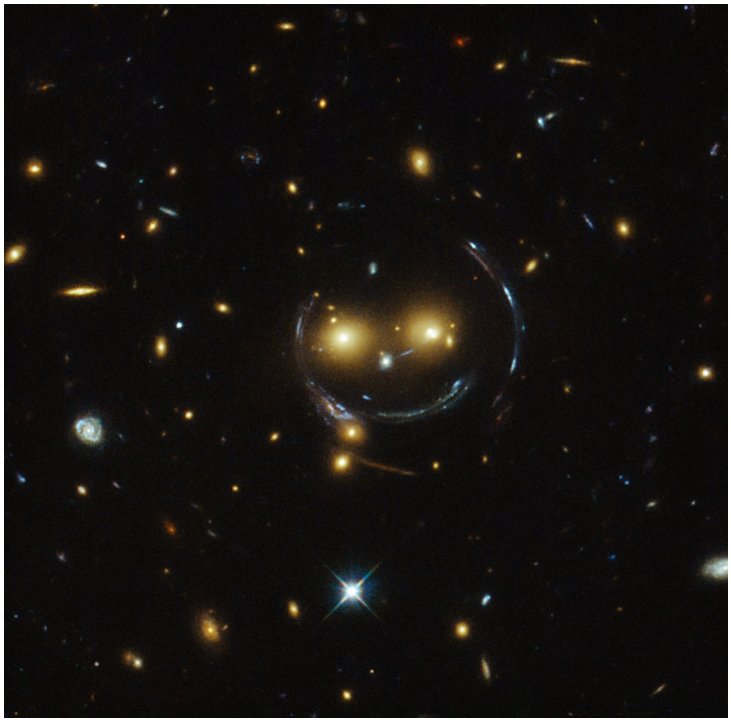

Figure 1.3: An example of gravitational lensing showing the "Cheshire Cat" image of galaxy cluster SDSS J1038+4849, taken by the Hubble Space Telescope. Figure taken from [20].

where $Y_{lm}(\theta, \phi)$ are spherical harmonics. The variance of a_{lm} is given by

$$C_l = \left\langle |a_{lm}|^2 \right\rangle = \frac{1}{2l+1} \sum_{m=-l}^{+l} |a_{lm}|. \tag{1.11}$$

As the temperature fluctuations appear to be Gaussian, all the information contained in the CMB anisotropy maps can be condensed into the power spectrum given by the behaviour of C_l as a function of l. This is generally represented using $D_l = l(l+1)C_l/2\pi$, as illustrated in Figure 1.5.

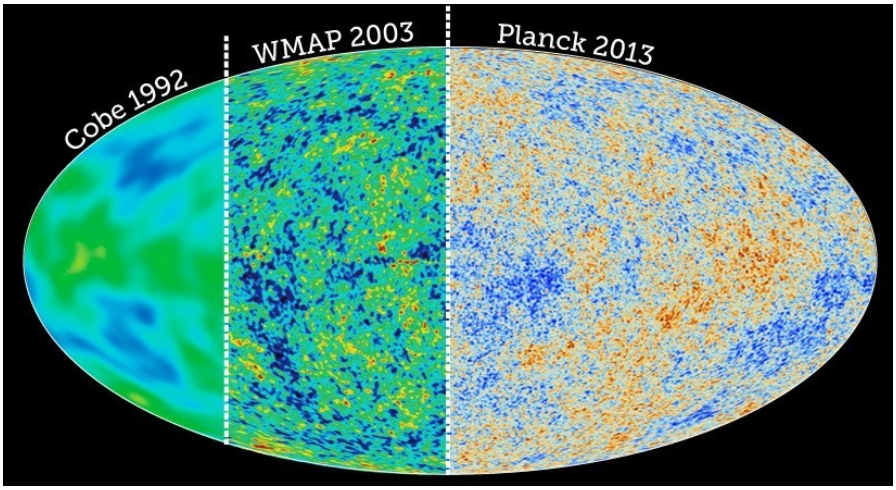

Figure 1.4: The CMB temperature fluctuations obtained from the COBE, WMAP, and Planck data. Figure taken from [25].

The CMB anisotropies are caused by acoustic oscillations arising from the conflict between the gravitational pull from baryons and dark matter and the repulsive force due to the radiation pressure from the photons. One popular model to describe and interpret the these observations is the ΛCDM model. CDM

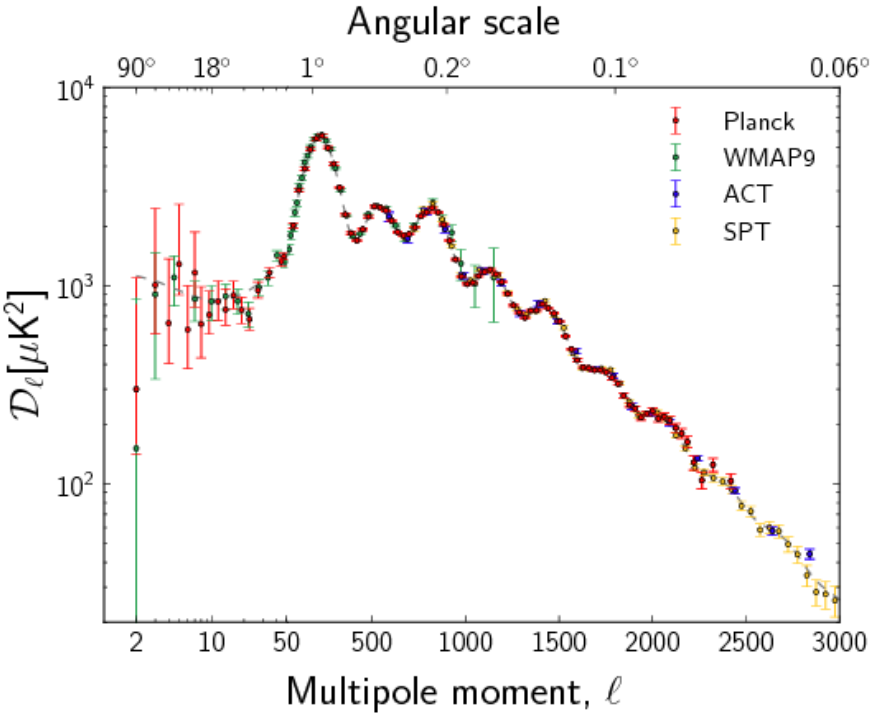

Figure 1.5: The observed power spectrum of the CMB anisotropies. The horizontal axis is logarithmic up to $l = 50$ and linear beyond. Figure taken from [26].

stands for cold dark matter, indicating that in this model the dark matter particles are moving slowly compared to the speed of light, while the Λ represents the cosmological constant, which is associated with the vacuum energy or dark energy that is used to explain the accelerating expansion of space. The ΛCDM model is compatible with a number of observations beyond the CMB fluctuations, such as the large scale structure in the distribution of galaxies, the relative abundance of light nuclei, and the accelerating expansion of the universe which is observed from the red shift of well-known spectral absorption or emission lines in the light of distant galaxies. Using this model to fit the power spectrum, the multiple peaks in the spectrum can be interpreted. The angular scale of the first peak can be used to determine the curvature of the universe. The second peak determines the reduced baryon density and the third peak can be used to retrieve information about the dark matter density. From the analysis of the Planck data the abundance of baryons and matter in the universe is determined to be

$$\Omega_b h^2 = 0.02205 \pm 0.00028 \qquad \Omega_M h^2 = 0.1423 \pm 0.0029 \tag{1.12}$$

This result shows that only about 15% of the matter in the universe is made up from the ordinary known matter, and the remaining 85% is called dark matter.

More evidence for dark matter was found from a great variety of data, both on subgalactic and intergalactic scales. Without discussing them here in detail, a few examples are the velocity dispersions of spiral galaxy satellites, suggesting the existence of dark halos around spiral galaxies extending well beyond the visible disk [27], the velocity dispersion of dwarf spheroidal galaxies, implying larger mass-to-light ratios than those observed in our local neighbourhood [28], and the so-called Oort discrepancy in the disk of the Milky Way, inferring the existence of dark matter from the inconsistency between the amount of stars in the solar neighbourhood and the gravitational potential indicated by their distribution [29].

1.2.2 Dark matter models

Since very little is know so far concerning the nature of dark matter, a multitude of dark matter candidates are discussed in the literature. Without attempting to be complete, a list is given and a few of the more popular candidates are briefly covered here.

Standard Model neutrinos

As mentioned before, the Standard Model could explain the existence of dark matter with the already observed neutrinos. However, it can be shown [30] that their total relic density is predicted to be

$$\Omega_\nu h^2 = \sum_{i=1}^{3} \frac{m_i}{93\ \mathrm{eV}}, \tag{1.13}$$

taking the sum over the 3 neutrino flavours. Currently, the most stringent upper bound on neutrino masses is

$$m_\nu < 2.05\ \mathrm{eV} \quad \text{at } 95\%\ \mathrm{CL} \tag{1.14}$$

obtained in tritium β-decay experiments at Troitsk [31, 32] and Mainz [33]. Since the mass difference between the 3 neutrinos must be very small to explain solar and atmospheric neutrino anomalies [34], this mass limit applies to the three mass eigenvalues, implying an upper bound on the total neutrino relic density of

$$\Omega_\nu h^2 \lesssim 0.07. \tag{1.15}$$

This shows that Standard Model neutrinos are not abundant enough to be the dominant component of dark matter.

Sterile neutrinos

Proposed in 1993 by Dodelson and Widrow [35], these hypothetical particles are similar to the Standard Model neutrinos, but without Standard Model weak interactions, except for mixing. The analysis of their cosmological abundance and the study of their decay products places stringent constraints on the sterile neutrinos. Light neutrinos with masses below a few keV would for example be ruled out [36].

Axions

These particles were originally introduced to solve the problem of the apparent absence of CP-violation by the strong interaction, and have often been discussed as dark matter candidates. They are expected to interact extremely weakly with Standard Model particles. Furthermore, observations from laboratory searches, stellar cooling, and the dynamics of supernova 1987A constrain the axion mass to be very small, of the order of or below 0.01 eV [37].

SUSY candidates

Several particles in supersymmetry (SUSY) models can serve as dark matter candidate, such as gravitinos and neutralinos. Gravitinos are the superpartners of the graviton. In some SUSY models, they can be the lightest supersymmetry particle and can be stable. While they are very strongly motivated theoretically, they are very difficult to observe, as they only interact gravitationally. The neutralinos are the superpartners of the photon, Z boson, and neutral Higgs bosons. The lightest of the four is stable and is an excellent dark matter candidate. These dark matter candidates are often called weakly interacting massive particles (WIMPs), since they are massive and interact through the weak interaction. As many SUSY models predict a new particle with the correct properties and self-annihilation cross section to obtain the correct abundance of dark matter today, a stable supersymmetric partner has long been a very plausible dark matter candidate and a lot of experimental effort has been made to detect it.

WIMPs

A prevalent assumption is that dark matter particles are a relic from the early universe, when all particles were in thermal equilibrium. At those high energies the dark matter particles and antiparticles could be formed by sufficiently energetic lighter particles, and they would annihilate back into these lighter particles as well. However, as the universe expanded and cooled down, the thermal energy of the lighter particles became insufficient to form dark matter particle-antiparticle pairs. The annihilation of the dark matter particles and antiparticles continued however, until the dark matter density decreased considerably and the interaction between the dark matter particles stopped. The

number of dark matter particles would remain constant from that moment on. In comparison, particles with a large interaction cross section would continue to annihilate for a longer period of time and would be less abundant.

The interaction cross section of the annihilating dark matter particles can be inferred from the current estimates of the dark matter abundance in the universe, and can in this case not be larger than the cross section of the weak interaction. According to this model, WIMPs would be the perfect candidates for dark matter. In general, they are hypothetical new elementary particles that interact gravitationally and through any other force which is as weak or weaker than the Standard Model weak interaction, and they could have been produced thermally as described in this model. Since WIMPs have a relatively large mass, they would also constitute cold dark matter, which would fit the observed large scale structure of the universe. The coincidence of WIMPs fitting so well into this model and corresponding to the current observations is known as the "WIMP miracle".

Many more dark matter candidates are discussed in literature, such as but not limited to heavy fourth generation neutrinos [38], Kaluza-Klein states in ADD [39] or RS [40] extra dimensions models, superheavy dark matter or Wimpzillas [41], self-interacting dark matter [42], charged massive particles (CHAMPs) [43], and Q-balls [44]. More detailed reviews are given in [30, 45, 46].

1.2.3 Detection of dark matter

The detection of dark matter can be categorised in three groups, based on the diagram shown in Figure 1.6. In the case of direct detection experiments, the studied process is the scattering of dark matter off ordinary matter. Experiments searching for dark matter with the indirect approach look for particles or radiation produced in the annihilation of dark matter particles. Finally, at collider experiments, attempts are made to produce and detect dark matter particles by colliding Standard Model particles at high energies.

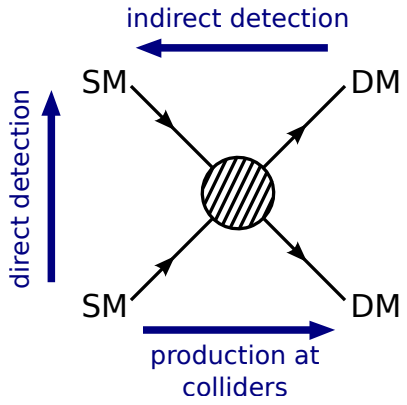

Figure 1.6: Diagram illustrating the three used methods to detect dark matter.

1.2.3.1 Direct detection experiments

This category of experiments is based on the fact that if our galaxy is filled with a static halo of dark matter particles, then many of them should pass through the Earth as it rotates around Galactic Center, and they could be detected by looking for the interaction of such particles with matter. This is for example done by recording the recoil energy of nuclei when WIMPs scatter off them. In order to determine the expected rate of events per unit detector material mass, the WIMP-nucleon scattering cross section and the density and velocity distribution of the WIMPs in the solar neighbourhood are needed.

There are several types of scattering processes which can be classified by two relevant characteristics: elastic or inelastic scattering and spin-dependent or spin-independent scattering. In the case of elastic scattering, the WIMP simply scatters off a nucleus as a whole, causing it to recoil. The recoil energy spectrum can then be measured by detecting the emitted scintillation light with very sensitive detectors

or by measuring very small temperature changes due to crystal vibrations. Taking a Maxwell-Boltzmann velocity distribution with as characteristic velocity our rotation velocity of about 270 km/s, the recoil spectrum is exponential with typical energies of $\langle E \rangle \sim 50$ keV. This range of energies is easily detectable by current experiments, which can detect recoils as low as 1-10 keV. Instead, when the WIMP scatters inelastically, it interacts with the orbital electrons of the target, exciting the electrons or ionising the target. Differently, the WIMP could also excite the target nuclei, which would then emit a photon about a nanosecond after the observed recoil. This signature has, however, to compete with the background from natural radioactivity.

The spin dependence or independence of the scattering depends on the coupling of the WIMPs to the Standard Model particles. Spin-dependent interactions result from couplings to the spin content of a nucleon, yielding cross sections that are proportional to J(J+1) instead of the number of nucleons. For spin-independent interactions, the cross section instead increases considerably with the mass of the target nuclei. The spin-independent scattering therefore dominates over the spin-dependent one in experiments which use heavy atoms.

Numerous direct detection experiments are currently operational or in development. They use one or more techniques to measure the nuclear recoil, by detecting the scintillation light, the change in temperature, or the ionisation. Some experiments also try to separate the WIMP signatures from the background by looking for an annual modulation in the rate, which arises due to the Earth's movement around the Sun. This effect causes the Earth to have a relative velocity with respect to the galaxy's reference frame, given by

$$v_E = 220\mathrm{km/s}\,(1.05 + 0.07\cos(2\pi(t - t_m)))\,, \tag{1.16}$$

where the time is in units of years and t_m is approximately the beginning of June. As a result, a small variation of about 7% in the WIMP flux can be measured in the direct detection rate.

Currently, there is some tension between the results obtained by the different experiments, as some observations can be interpreted as dark matter signals, while other experiments are ruling out those models. The DAMA experiment for example observes an annual modulation in the event rate, pointing to the existence of WIMPs scattering elastically off the sodium and iodine nuclei in the detector [47]. Other experiments, such as SuperCDMS [48], EDELWEISS-III [49], CRESST-II [50], XENON100 [51], have seen no evidence for dark matter so far and placed limits on many dark matter models, creating a tension with the observed signal at DAMA. For WIMP masses above a few GeV, the strongest limit of direct detection experiments for spin-independent interactions is currently given by LUX [52]. For a spin-dependent WIMP-proton cross section, the most stringent limit is set by the PICO experiment [53], while the PandaX experiment places the strongest limit on the WIMP-neutron cross section [54]. An overview of the existing limits and signal observations is given in Figure 1.7, showing the mentioned experiments, and a more complete review of the existing direct detection results is given in [55].

1.2.3.2 Indirect detection experiments

The indirect detection of dark matter is performed by looking for radiation produced in dark matter annihilations. A reasonable place to look at would then be in regions with large dark matter densities and thus larger annihilation rates, which will result in a higher flux of the studied radiation. Some examples are dense regions of the galactic halo such as the galactic centre, or objects like the Sun or the Earth, which could also capture dark matter particles through scattering with nucleons in their core. In the latter case, only neutrinos would be able to escape those dense objects. Other annihilation products include gamma rays, positrons, and antiprotons.

In order to observe gamma rays directly, the detectors must be placed in space, as photons of the relevant energy range (GeV to TeV) interact with matter via e^+e^- pair production and cannot traverse more than a surface density of about 38 g cm^{-2}. The gamma rays will not reach the ground-based telescopes as the Earth's atmosphere is 1030 g cm^{-2} thick. Nevertheless, efforts are being made to observe gamma rays indirectly via ground-based experiments as well, by detecting the secondary particles and the Cherenkov light produced by their passage through the Earth's atmosphere. In the energy range between approximately 100 MeV and 100 GeV, gamma ray telescopes on satellites such as the Fermi

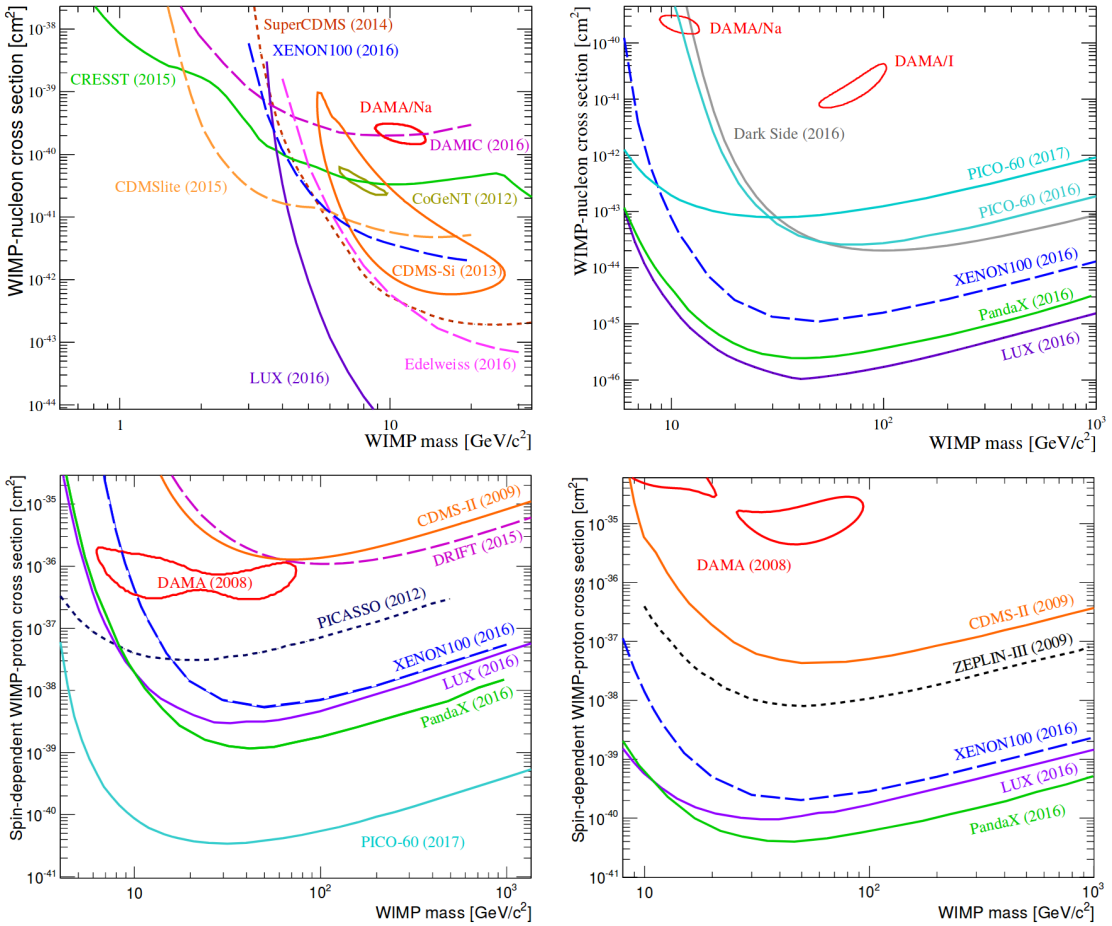

Figure 1.7: Overview of the current limits for spin-independent WIMP-nucleon interactions at low (top left) and high (top right) WIMP masses, spin-dependent WIMP-proton interactions (bottom left), and spin-dependent WIMP-neutron interactions (bottom right). The observed signals from DAMA, CoGeNT, and CDMS-Si are shown as well. Figure taken from [55].

Large Area Telescope [56] are being used. Above 100 GeV, the ground-based Imaging Air Cherenkov Telescopes such as HESS [57], MAGIC [58], and VERITAS [59] become more adequate.

Neutrinos can also be produced in the annihilation of dark matter particles, but they are considerably more difficult to detect than gamma rays due to their weak interaction with ordinary matter. They are not easily absorbed, which makes it possible to observe them with underground, low-background experiments. Very energetic neutrinos, in the GeV-TeV range, are most easily observed by detecting the Cherenkov light from muons produced through charge current interactions of the neutrinos inside of or close to the detector volume. Two very large neutrino detectors are ANTARES in the Mediterranean Sea [60] and IceCube at the South Pole [61].

Additionally, evidence for dark matter annihilations can also be found by studying the spectra of cosmic positrons and antiprotons. Contrary to neutrinos and gamma rays, these charged particles do not point to their source, as their trajectory is modified by the presence of galactic magnetic fields. Currently, the main detector for positrons and antiprotons is AMS [62], which is operating on the International Space Station. Until 2016, PAMELA [63] was also active on board of the Resurs-DK1 satellite.

Finally, radio emissions from the galactic halo, and in particular from the galactic centre, can also provide evidence for dark matter annihilation. Electrons and protons produced in dark matter annihilations will emit synchrotron radiation at radio wavelengths as they move through galactic magnetic fields. This type of searches is performed with radio telescopes and belongs to the realm of classical astronomy.

1.2.3.3 Collider experiments

Since dark matter particles are usually assumed to be neutral and to interact only weakly with ordinary matter, they are expected to pass through the detectors at colliders without leaving a signal, similar to neutrinos. These particles can however still be searched for at colliders as well, when they are produced in association with other visible particles which are detected as jets or charged leptons. The dark matter particles are then observed as missing energy, as they create an imbalance in the net momentum in the transverse plane perpendicular to the colliding beams, which should be zero. One of these flagship analyses is the monojet analysis, looking for dark matter produced together with one or more jets [64, 65]. Similarly, many more searches are performed at the CMS and ATLAS experiments at the LHC by looking for signatures containing missing energy. Recent summaries are given in [66] and [67].

Additionally, other signatures without missing energy can also be used to search for dark matter. If the dark matter particle is produced in a cascade of decays for example, different signatures can be obtained, such as displaced vertices [68], disappearing tracks [69], and displaced lepton-jets [70]. Furthermore, in dijet searches [71–73], resonances in the mass spectrum are being looked for, as this could point to the existence of a new dark matter mediator. If the dark matter particles couple to quarks via a dark matter mediator, this mediator can either decay to a pair of dark matter particles or a pair of Standard model quarks which can be observed as a pair of jets. Finally, for some particular types of dark matter candidates, such as strongly interacting massive particles (SIMPs) [74] or heavy stable neutral particles (HSCPs) [75, 76], more unusual signatures are expected. This is currently a developing area of dark matter research, and more and more searches looking for new signatures are appearing.

In Figures 1.8 and 1.9, recent limits from dark matter searches at the CMS experiment are compared to the direct detection results, for spin-dependent and spin-independent interactions, respectively.

1.3 Strongly Interacting Massive Particles

As no observation of dark matter has been made so far, despite many searches probing the more popular models described in the previous section, many scenarios now venture beyond minimal models or give up basic assumptions for the WIMP. In the following model, which is studied in this thesis, the interaction cross section of the dark matter with normal matter is so high that the particles are no longer WIMPs, but so-called strongly interacting massive particles (SIMPs). This model can also be motivated by the long lasting interest for self-interacting dark matter (SIDM)[4] particles with a large cross section [42], which could help to explain observations that present a challenge for the cold dark matter scenarios, such as the missing satellites or core-cusp problems [78–81]. While it is possible to create models with a strongly interacting hidden sector that is weakly coupled to the Standard Model particles, SIDM particles that interact rather strongly with the known matter particles can be considered as well.

1.3.1 The SIMP simplified model

In this simplified model, the dark matter particles χ can be produced at the LHC in pairs, through a new strong interaction with a new mediator ϕ, as illustrated in Figure 1.10. These SIMPs are neutral and stable, and are generated off-shell as the mediator is very light, of the order of the pion mass: $m_\phi = 140$ MeV. We only consider the case of fermionic candidates, since the bosonic form is ruled out by constraints coming from neutron stars and black holes, as is described in Section 1.3.2. Both the cases with a scalar or a vector mediator can be studied, and the corresponding interaction Lagrangian is

$$\mathcal{L}_{\text{int}} = \begin{cases} -g_\chi \phi \bar{\chi}\chi - g_q \phi \bar{q} q & \text{(scalar mediator)} \\ -\tilde{g}_\chi \phi_\mu \bar{\chi}\gamma^\mu \chi - \tilde{g}_q \phi_\mu \bar{q}\gamma^\mu q & \text{(vector mediator)} \end{cases} \tag{1.17}$$

with $g_\chi g_q, \tilde{g}_\chi \tilde{g}_q < 0$ to avoid the formation of bound states. For simplicity we assume that the SIMPs have a universal coupling to quarks, although a flavour dependent coupling could be preferred, as light SIMPs with a significant coupling to b or c quarks are probably constrained by B and D meson phenomenology.

[4] Incidentally, self-interacting and strongly interacting share the same abbreviation, such that SIDM can also stand for strongly interacting dark matter and SIMP for self-interacting massive particles in the literature.

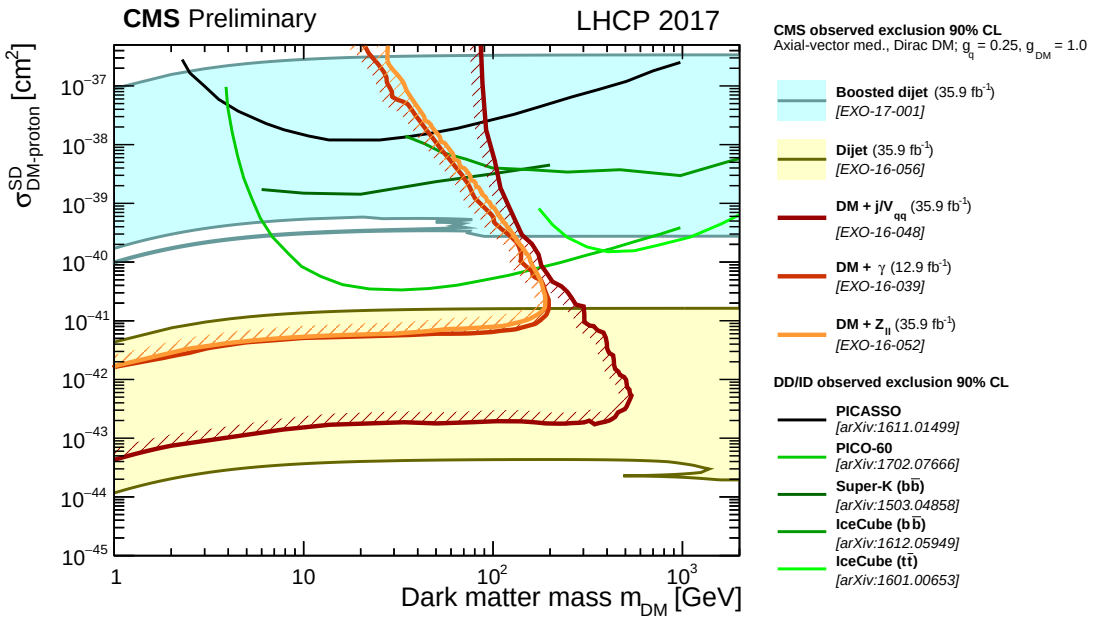

Figure 1.8: A comparison of CMS results to direct detection experiments in the $\mathrm{m_{DM}} - \sigma_{\mathrm{SD}}$ plane. The limits are shown at 90% CL. The shown CMS contours are for an axial-vector mediator with Dirac dark matter and couplings $g_q = 0.25$ and $g_{\mathrm{DM}} = 1.0$. The spin-dependent exclusion contours are compared with limits from the PICASSO and PICO experiments, the IceCube limit for the $t\bar{t}$ and $b\bar{b}$ annihilation channels, and the Super-Kamiokande limit for the $b\bar{b}$ annihilation channel. It should be noted that the CMS limits do not include a constraint on the relic density and also the absolute exclusion of the different CMS searches as well as their relative importance will strongly depend on the chosen coupling and model scenario. Therefore, the shown CMS exclusion regions in this plot are not applicable to other choices of coupling values or models. Figure taken from [77].

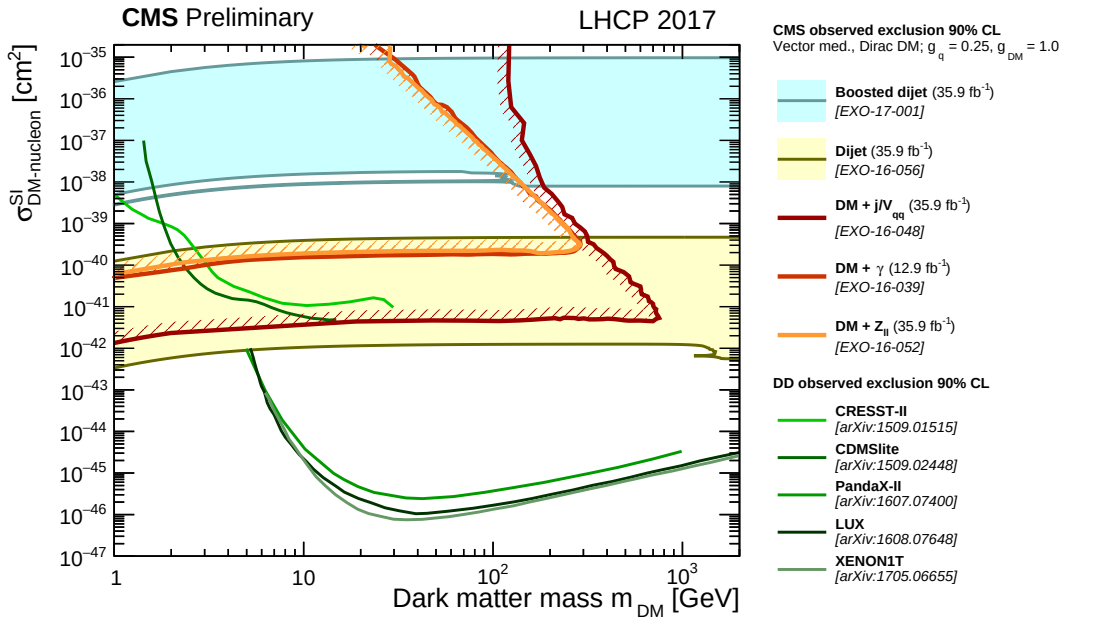

Figure 1.9: A comparison of CMS results to direct detection experiments in the $\mathrm{m_{DM}} - \sigma_{\mathrm{SI}}$ plane. The limits are shown at 90% CL. The shown CMS contours are for a vector mediator with Dirac dark matter and couplings $g_q = 0.25$ and $g_{\mathrm{DM}} = 1.0$. The spin-independent exclusion contours are compared with the XENON1T 2017, LUX 2016, PandaX-II 2016, CDMSLite 2015 and CRESST-II 2015 limits, which constitutes the strongest documented constraints in the shown mass range. It should be noted that the CMS limits do not include a constraint on the relic density and also the absolute exclusion of the different CMS searches as well as their relative importance will strongly depend on the chosen coupling and model scenario. Therefore, the shown CMS exclusion regions in this plot are not applicable to other choices of coupling values or models. Figure taken from [77].

SIMPs lighter than about 5 GeV could for example appear in the decay of b or c quarks, and would be constrained by limits on the invisible decay of B and D mesons.

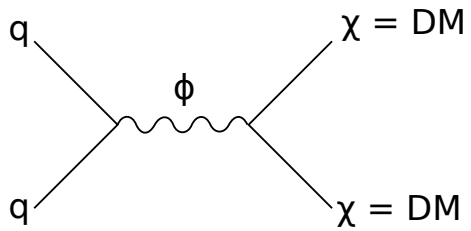

Figure 1.10: Feynman diagram showing the production of a SIMP pair, through a new low-mass mediator.

Introducing a new strong interaction between quarks can however modify nuclear potentials. In order to keep the impact small, the mediator is assumed to not modify nuclear potentials by more than $\mathcal{O}(10\%)$, such that $g_{\chi N} \lesssim 0.3 g_{\pi NN} \sim 3$ for a mediator with the mass of a pion, where $g_{\pi NN} \sim 13$ is the effective pseudoscalar pion-nucleon coupling [82]. The quoted values are however not very precise, as a large spread of values can be found in the literature for meson-nucleon effective couplings, sometimes differing by a factor 2 or more (see e.g. [83] for comparison). This shows the difficulty of dealing with strong interactions in the framework of effective field theories, which arise because contributions from many mesons need to be taken into account, each of them with a different coupling. No constraints on modified strong interactions at low energies seem to exist in literature so far, however searches at fixed-target experiments do place constraints on the existence of strongly interacting stable neutral particles.

In summary, the model has 4 free parameters: the two couplings, the mass of the mediator m_ϕ, and the mass of the SIMP m_χ. At the LHC, only the product of the couplings appears, while astrophysical observations constrain both the dark matter self-interaction and the interaction with the Standard Model.

1.3.2 Experimental constraints

Naively, one would expect such an unusual model with strong interactions not to be viable, as various types of experiments and observations set constraints on SIMPs as dark matter candidates. However, some of these limitations can be avoided by the assumptions in the model described above. The relevant existing measurements are described below, showing there is a still a part of phase space which remained unexplored so far.

Bound states

Searches for heavy isotopes, in particular heavy water, constrain the formation of bound states between SIMPs and nucleons, ruling out particles with a mass below 10 TeV for the scenario with SIMPs as dominant contribution to dark matter. This constraint is evaded by assuming a purely repulsive SIMP-nucleon interaction with opposite sign couplings, as is specified in the Lagrangian (1.17). In the vector mediator case, vector mediators would however couple to the dark matter antiparticles with an opposite charge. This is avoided if no dark matter antiparticles are around, i.e. if the abundance of dark matter is asymmetric. A reason for having asymmetric SIMPs is that if they are the dominant source of dark matter, then the dark matter abundance is set by either an asymmetry or through a non-thermal mechanism. In the case of a symmetric SIMP candidate, the dark matter abundance is determined by thermal freeze-out, and it can only be a sub-dominant component. Additional constraints also exist on the dark matter self-interacting strength from halo shapes and merging galaxies such as the Bullet cluster [84, 85].

Earth heating

A second argument for an asymmetric abundance of SIMPs comes from experiments measuring the heat emitted from the Earth's core. For the typical SIMPs cross sections, the dark matter particles can be captured by the Earth and accumulate in its core over time. Annihilating SIMPs would then

provide a substantial source of heat and could modify the Earth's heat flow. This can be measured by detectors in deep underground shafts [86] and rules out the scenario with symmetric SIMPs.

Neutron stars and black holes

In the asymmetric scenario, light scalar dark matter particles can however be collected in the cores of neutron stars and cause them to collapse into black holes. Bosonic dark matter candidates are therefore excluded, and we consider only fermionic candidates as mentioned previously.

Direct detection searches

Many bounds on the SIMP parameter space also come from the direct detection searches. Underground experiments, such as CDMS and XENON, place strong constraints at smaller cross sections, about 5 orders of magnitude below the SIMP cross section, as can be seen from Figure 1.11. At the higher cross sections considered here, the SIMPs are stopped by the Earth's atmosphere, and they cannot reach the underground detectors. At higher altitudes however, space or airborne experiments such as RSS [87], a balloon-based experiment with a silicon semiconductor detector, and XQC [88], a sounding rocket experiment, exclude SIMPs in some regions of phase space. More details on these constraints can be found in [86], where they have been extensively reviewed.

Nucleosynthesis and cosmic rays

There are also bounds from primordial nucleosynthesis and cosmic rays, reviewed in [89] and [90]. The protons in cosmic rays can scatter off dark matter particles and create neutral pions, which decay to photons and could be detected in gamma ray telescopes. Although limits have been placed on dark matter-nucleon interactions [90], these constraints depend on many assumptions and adopt a form of the dark matter density near the galactic core. Since the considered model describes a nonstandard form of dark matter with a relatively strong interaction with baryons, these densities may be considerably different.

CMB and large scale structure

Observations of the CMB anisotropies and the large scale structure power spectrum, including from the Lyman-α data [91, 92] additionally also place strong constraints on interactions between dark matter and baryons.

Fixed-target experiments

Finally, a relatively old fixed-target experiment led in 1976 at FNAL with a beam of neutral particles produced by 300 GeV protons hitting a beryllium target was used to look for massive, strongly interacting, neutral particles [93]. The mass of the particles was determined using their flight time and their kinetic energy which was measured in a calorimeter. Neutral particles with a mass larger than 2 GeV were searched for, in order to discriminate the candidates from the background of neutrons and lighter hadronic states, up to $m_\chi \lesssim \sqrt{E/2} \approx 12$ GeV, limited by the beam energy of $E = 300$ GeV. Single particle production was considered, but the results apply to pair production as well when they are translated into the case where 2 neutral particles are boosted and fly away in the same direction. The search showed no significant excess above the expected background and limits were placed on the invariant production cross section per nucleon versus the neutral particle interaction cross section. As an example, for an interaction cross section of 1 mb, a limit on the total production cross section of about $2.5 \times 10^{-35}\ \mathrm{cm}^2 = 25$ pb is found, and this limit is reported by the Particle Data Group [94]. Comparing the considered SIMP model to this result by simulating the pair production at $\sqrt{s} = 25$ GeV, one can conclude that SIMPs between 2 and about 6 GeV are already excluded by this experiment [95].

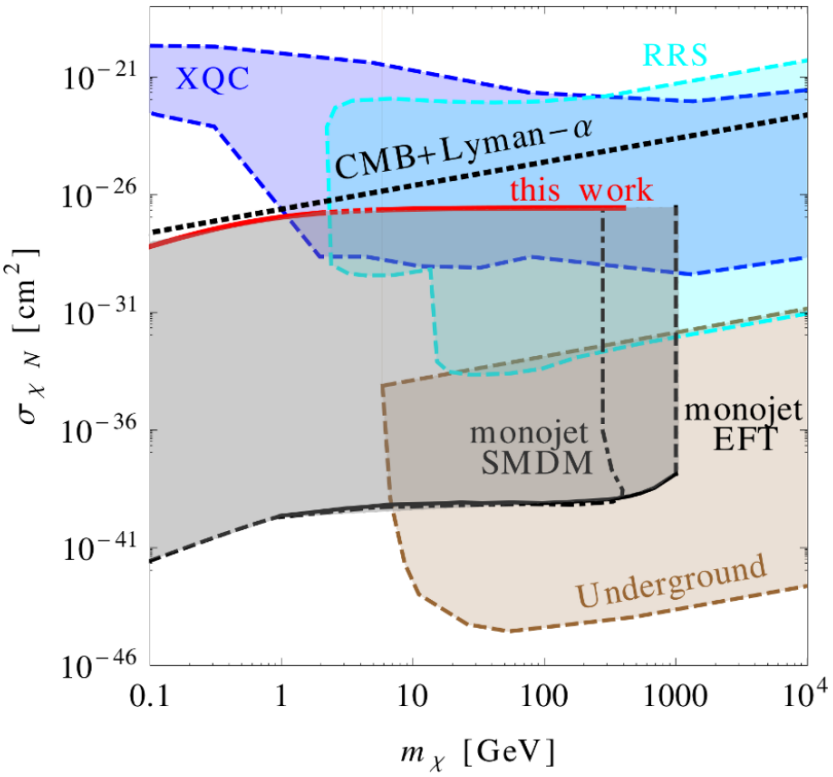

Figure 1.11: Summary plot showing the SIMP model (red) in comparison with the most important applicable constraints, coming from the LHC monojet analyses (black), the atmospheric XQC and RRS experiments (blue), underground experiments (brown), and the CMB observations and Lyman-α data (black dashed line). Figure taken from [95].

Bibliography

[1] Michael E Peskin and Daniel V Schroeder. *An introduction to quantum field theory; 1995 ed.* Westview, Boulder, CO, 1995.

[2] Yorikiyo Nagashima. *Beyond the standard model of elementary particle physics*. Wiley-VCH Verlag, Weinheim, Germany, 2014.

[3] Georges Aad et al. *Observation of a new particle in the search for the Standard Model Higgs boson with the ATLAS detector at the LHC*. Phys. Lett., B716:1–29, 2012.

[4] Serguei Chatrchyan et al. *Observation of a new boson at a mass of 125 GeV with the CMS experiment at the LHC*. Phys. Lett., B716:30–61, 2012.

[5] Sheldon L. Glashow. *The renormalizability of vector meson interactions*. Nucl. Phys., 10:107–117, 1959.

[6] Steven Weinberg. *A Model of Leptons*. Phys. Rev. Lett., 19:1264–1266, 1967.

[7] Abdus Salam and John Clive Ward. *Weak and electromagnetic interactions*. Nuovo Cim., 11:568–577, 1959.

[8] Peter W. Higgs. *Broken Symmetries and the Masses of Gauge Bosons*. Phys. Rev. Lett., 13:508–509, 1964.

[9] F. Englert and R. Brout. *Broken Symmetry and the Mass of Gauge Vector Mesons*. Phys. Rev. Lett., 13:321–323, 1964.

[10] G. S. Guralnik, C. R. Hagen, and T. W. B. Kibble. *Global Conservation Laws and Massless Particles*. Phys. Rev. Lett., 13:585–587, 1964.

[11] David J. Gross and Frank Wilczek. *Ultraviolet Behavior of Nonabelian Gauge Theories*. Phys. Rev. Lett., 30:1343–1346, 1973.

[12] H. David Politzer. *Reliable Perturbative Results for Strong Interactions?* Phys. Rev. Lett., 30:1346–1349, 1973.

[13] `http://www.quantumdiaries.org/2014/03/14/the-standard-model-a-beautiful-but-flawe`

[14] Q. R. Ahmad et al. *Direct evidence for neutrino flavor transformation from neutral current interactions in the Sudbury Neutrino Observatory*. Phys. Rev. Lett., 89:011301, 2002.

[15] Y. Fukuda et al. *Evidence for oscillation of atmospheric neutrinos*. Phys. Rev. Lett., 81:1562–1567, 1998.

[16] Gianfranco Bertone, Dan Hooper, and Joseph Silk. *Particle dark matter: Evidence, candidates and constraints*. Phys. Rept., 405:279–390, 2005.

[17] F. Zwicky. *Die Rotverschiebung von extragalaktischen Nebeln*. Helv. Phys. Acta, 6:110–127, 1933. [Gen. Rel. Grav.41,207(2009)].

[18] P. Salucci and A. Borriello. *The intriguing distribution of dark matter in galaxies*. Lect. Notes Phys., 616:66–77, 2003.

[19] K. G. Begeman, A. H. Broeils, and R. H. Sanders. *Extended rotation curves of spiral galaxies: Dark haloes and modified dynamics*. Mon. Not. Roy. Astron. Soc., 249:523, 1991.

[20] V. Belokurov, N. W. Evans, P. C. Hewett, A. Moiseev, R. G. McMahon, S. F. Sanchez, and L. J. King. *Two New Large Separation Gravitational Lenses from SDSS*. Mon. Not. Roy. Astron. Soc., 392:104, 2009.

[21] Arno A. Penzias and Robert Woodrow Wilson. *A Measurement of excess antenna temperature at 4080-Mc/s*. Astrophys. J., 142:419–421, 1965.

[22] George F. Smoot et al. *Structure in the COBE differential microwave radiometer first year maps*. Astrophys. J., 396:L1–L5, 1992.

[23] E. Komatsu et al. *Seven-Year Wilkinson Microwave Anisotropy Probe (WMAP) Observations: Cosmological Interpretation*. Astrophys. J. Suppl., 192:18, 2011.

[24] P. A. R. Ade et al. *Planck 2013 results. XVI. Cosmological parameters*. Astron. Astrophys., 571:A16, 2014.

[25] `https://briankoberlein.com/2015/06/15/science-in-the-raw/`.

[26] P. A. R. Ade et al. *Planck 2013 results. I. Overview of products and scientific results*. Astron. Astrophys., 571:A1, 2014.

[27] M. Azzaro, F. Prada, and C. M. Gutierrez. *Motion properties of satellites around external spiral galaxies*. ASP Conf. Ser., 327:268, 2004.

[28] Mario Mateo. *Dwarf galaxies of the Local Group*. Ann. Rev. Astron. Astrophys., 36:435–506, 1998.

[29] John N. Bahcall, Chris Flynn, and Andrew Gould. *Local dark matter from a carefully selected sample*. Astrophys. J., 389:234–250, 1992.

[30] Lars Bergstrm. *Nonbaryonic dark matter: Observational evidence and detection methods*. Rept. Prog. Phys., 63:793, 2000.

[31] V. M. Lobashev. *The search for the neutrino mass by direct method in the tritium beta-decay and perspectives of study it in the project KATRIN*. Nucl. Phys., A719:153–160, 2003.

[32] V. N. Aseev et al. *An upper limit on electron antineutrino mass from Troitsk experiment*. Phys. Rev., D84:112003, 2011.

[33] Ch. Kraus et al. *Final results from phase II of the Mainz neutrino mass search in tritium beta decay*. Eur. Phys. J., C40:447–468, 2005.

[34] M. C. Gonzalez-Garcia and Yosef Nir. *Neutrino masses and mixing: Evidence and implications*. Rev. Mod. Phys., 75:345–402, 2003.

[35] Scott Dodelson and Lawrence M. Widrow. *Sterile-neutrinos as dark matter*. Phys. Rev. Lett., 72:17–20, 1994.

[36] Naoki Yoshida, Aaron Sokasian, Lars Hernquist, and Volker Springel. *Early structure formation and reionization in a warm dark matter cosmology*. Astrophys. J., 591:L1–L4, 2003.

[37] L. J. Rosenberg and K. A. van Bibber. *Searches for invisible axions*. Phys. Rept., 325:1–39, 2000.

[38] Kimmo Kainulainen and Keith A. Olive. *Astrophysical and cosmological constraints on neutrino masses*. Springer Tracts Mod. Phys., 190:53–74, 2003.

[39] Nima Arkani-Hamed, Savas Dimopoulos, and G. R. Dvali. *The Hierarchy problem and new dimensions at a millimeter*. Phys. Lett., B429:263–272, 1998.

[40] Lisa Randall and Raman Sundrum. *A Large mass hierarchy from a small extra dimension*. Phys. Rev. Lett., 83:3370–3373, 1999.

[41] Edward W. Kolb, Daniel J. H. Chung, and Antonio Riotto. *WIMPzillas!* In Trends in theoretical physics II. Proceedings, 2nd La Plata Meeting, Buenos Aires, Argentina, November 29-December 4, 1998, pages 91–105, 1998. [,91(1998)].

[42] David N. Spergel and Paul J. Steinhardt. *Observational evidence for selfinteracting cold dark matter*. Phys. Rev. Lett., 84:3760–3763, 2000.

[43] A. De Rujula, S. L. Glashow, and U. Sarid. *CHARGED DARK MATTER*. Nucl. Phys., B333:173–194, 1990.

[44] Alexander Kusenko and Mikhail E. Shaposhnikov. *Supersymmetric Q balls as dark matter*. Phys. Lett., B418:46–54, 1998.

[45] John R. Ellis. *Particle candidates for dark matter*. Phys. Scripta, T85:221–230, 2000.

[46] Lars Bergstrom. *Dark Matter Candidates*. New J. Phys., 11:105006, 2009.

[47] R. Bernabei et al. *Final model independent result of DAMA/LIBRA-phase1*. Eur. Phys. J., C73:2648, 2013.

[48] R. Agnese et al. *Search for Low-Mass Weakly Interacting Massive Particles with SuperCDMS*. Phys. Rev. Lett., 112(24):241302, 2014.

[49] E. Armengaud et al. *Constraints on low-mass WIMPs from the EDELWEISS-III dark matter search*. JCAP, 1605(05):019, 2016.

[50] G. Angloher et al. *Results on low mass WIMPs using an upgraded CRESST-II detector*. Eur. Phys. J., C74(12):3184, 2014.

[51] E. Aprile et al. *XENON100 Dark Matter Results from a Combination of 477 Live Days*. Phys. Rev., D94(12):122001, 2016.

[52] D. S. Akerib et al. *Results from a search for dark matter in the complete LUX exposure*. Phys. Rev. Lett., 118(2):021303, 2017.

[53] C. Amole et al. *Dark Matter Search Results from the PICO-60 C_3F_8 Bubble Chamber*. Phys. Rev. Lett., 118(25):251301, 2017.

[54] Changbo Fu et al. *Spin-Dependent Weakly-Interacting-Massive-ParticleNucleon Cross Section Limits from First Data of PandaX-II Experiment*. Phys. Rev. Lett., 118(7):071301, 2017.

[55] Teresa Marrodn Undagoitia and Ludwig Rauch. *Dark matter direct-detection experiments*. J. Phys., G43(1):013001, 2016.

[56] W. B. Atwood et al. *The Large Area Telescope on the Fermi Gamma-ray Space Telescope Mission*. Astrophys. J., 697:1071–1102, 2009.

[57] F. Aharonian et al. *Observations of the Crab Nebula with H.E.S.S.* Astron. Astrophys., 457:899–915, 2006.

[58] J. Aleksic et al. *Performance of the MAGIC stereo system obtained with Crab Nebula data*. Astropart. Phys., 35:435–448, 2012.

[59] J. Holder et al. *Status of the VERITAS Observatory*. AIP Conf. Proc., 1085:657–660, 2009.

[60] M. Ageron et al. *ANTARES: the first undersea neutrino telescope*. Nucl. Instrum. Meth., A656:11–38, 2011.

[61] A. Achterberg et al. *First Year Performance of The IceCube Neutrino Telescope*. Astropart. Phys., 26:155–173, 2006.

[62] Andrei Kounine. *The Alpha Magnetic Spectrometer on the International Space Station*. Int. J. Mod. Phys., E21(08):1230005, 2012.

[63] P. Picozza et al. *PAMELA: A Payload for Antimatter Matter Exploration and Light-nuclei Astrophysics*. Astropart. Phys., 27:296–315, 2007.

[64] Albert M Sirunyan et al. *Search for dark matter produced with an energetic jet or a hadronically decaying W or Z boson at* $\sqrt{s} = 13$ *TeV*. JHEP, 07:014, 2017.

[65] Morad Aaboud et al. *Search for dark matter produced in association with a hadronically decaying vector boson in pp collisions at* $\sqrt{s} = 13$ *TeV with the ATLAS detector*. Phys. Lett., B763:251–268, 2016.

[66] Felix Kahlhoefer. *Review of LHC Dark Matter Searches*. Int. J. Mod. Phys., A32(13):1730006, 2017.

[67] Oliver Buchmueller, Caterina Doglioni, and Lian Tao Wang. *Search for dark matter at colliders*. Nature Phys., 13(3):217–223, 2017.

[68] The ATLAS collaboration. *Search for long-lived, massive particles in events with displaced vertices and missing transverse momentum in 13 TeV pp collisions with the ATLAS detector*. 2017.

[69] The ATLAS collaboration. *Search for long-lived charginos based on a disappearing-track signature in pp collisions at* $\sqrt{s} = 13$ *TeV with the ATLAS detector*. 2017.

[70] The ATLAS collaboration. *Search for Higgs boson decays to Beyond-the-Standard-Model light bosons in four-lepton events with the ATLAS detector at* $\sqrt{s} = 13$ *TeV*. 2017.

[71] Albert M Sirunyan et al. *Search for new physics with dijet angular distributions in proton-proton collisions at* $\sqrt{s} = 13$ *TeV*. JHEP, 07:013, 2017.

[72] Albert M Sirunyan et al. *Search for dijet resonances in protonproton collisions at* $\sqrt{s}$ *= 13 TeV and constraints on dark matter and other models*. Phys. Lett., B769:520–542, 2017. [Erratum: Phys. Lett.B772,882(2017)].

[73] Morad Aaboud et al. *Search for new phenomena in dijet events using 37 fb*$^{-1}$ *of pp collision data collected at* $\sqrt{s}$ *=13 TeV with the ATLAS detector*. Phys. Rev., D96:052004, 2017.

[74] Yang Bai and Arvind Rajaraman. *Dark Matter Jets at the LHC*. 2011.

[75] CMS Collaboration. *Search for heavy stable charged particles with* $12.9\ \mathrm{fb}^{-1}$ *of 2016 data*. 2016.

[76] Morad Aaboud et al. *Search for metastable heavy charged particles with large ionization energy loss in pp collisions at* $\sqrt{s} = 13$ *TeV using the ATLAS experiment*. Phys. Rev., D93(11):112015, 2016.

[77] `http://cms-results.web.cern.ch/cms-results/public-results/publications/EXO/index.html`.

[78] James S. Bullock. *Notes on the Missing Satellites Problem*. 2010.

[79] Michael Boylan-Kolchin, James S. Bullock, and Manoj Kaplinghat. *Too big to fail? The puzzling darkness of massive Milky Way subhaloes*. Mon. Not. Roy. Astron. Soc., 415:L40, 2011.

[80] David H. Weinberg, James S. Bullock, Fabio Governato, Rachel Kuzio de Naray, and Annika H. G. Peter. *Cold dark matter: controversies on small scales*. Proc. Nat. Acad. Sci., 112:12249–12255, 2014. [Proc. Nat. Acad. Sci.112,2249(2015)].

[81] Benoit Famaey and Stacy McGaugh. *Challenges for Lambda-CDM and MOND*. J. Phys. Conf. Ser., 437:012001, 2013.

[82] J. F. Donoghue, E. Golowich, and Barry R. Holstein. *Dynamics of the standard model*. Camb. Monogr. Part. Phys. Nucl. Phys. Cosmol., 2:1–540, 1992. [Camb. Monogr. Part. Phys. Nucl. Phys. Cosmol.35(2014)].

[83] C. Downum, T. Barnes, J. R. Stone, and E. S. Swanson. *Nucleon-meson coupling constants and form-factors in the quark model*. Phys. Lett., B638:455–460, 2006.

[84] Scott W. Randall, Maxim Markevitch, Douglas Clowe, Anthony H. Gonzalez, and Marusa Bradac. *Constraints on the Self-Interaction Cross-Section of Dark Matter from Numerical Simulations of the Merging Galaxy Cluster 1E 0657-56*. Astrophys. J., 679:1173–1180, 2008.

[85] Jonathan L. Feng. *Dark Matter Candidates from Particle Physics and Methods of Detection*. Ann. Rev. Astron. Astrophys., 48:495–545, 2010.

[86] Gregory D. Mack, John F. Beacom, and Gianfranco Bertone. *Towards Closing the Window on Strongly Interacting Dark Matter: Far-Reaching Constraints from Earth's Heat Flow*. Phys. Rev., D76:043523, 2007.

[87] J. Rich, R. Rocchia, and M. Spiro. *A Search for Strongly Interacting Dark Matter*. Phys. Lett., B194:173, 1987. [,221(1987)].

[88] Adrienne L. Erickcek, Paul J. Steinhardt, Dan McCammon, and Patrick C. McGuire. *Constraints on the Interactions between Dark Matter and Baryons from the X-ray Quantum Calorimetry Experiment*. Phys. Rev., D76:042007, 2007.

[89] Gregory D. Mack and Adithya Manohar. *Closing the window on high-mass strongly interacting dark matter*. J. Phys., G40:115202, 2013.

[90] Richard H. Cyburt, Brian D. Fields, Vasiliki Pavlidou, and Benjamin D. Wandelt. *Constraining strong baryon dark matter interactions with primordial nucleosynthesis and cosmic rays*. Phys. Rev., D65:123503, 2002.

[91] Xue-lei Chen, Steen Hannestad, and Robert J. Scherrer. *Cosmic microwave background and large scale structure limits on the interaction between dark matter and baryons*. Phys. Rev., D65:123515, 2002.

[92] Cora Dvorkin, Kfir Blum, and Marc Kamionkowski. *Constraining Dark Matter-Baryon Scattering with Linear Cosmology*. Phys. Rev., D89(2):023519, 2014.

[93] H. Richard Gustafson, Cyril A. Ayre, Lawrence W. Jones, Michael J. Longo, and P. V. Ramana Murthy. *Search for New Massive Long-lived Neutral Particles*. Phys. Rev. Lett., 37:474, 1976.

[94] K. A. Olive et al. *Review of Particle Physics*. Chin. Phys., C38:090001, 2014.

[95] N. Daci, Isabelle De Bruyn, S. Lowette, M. H. G. Tytgat, and B. Zaldivar. *Simplified SIMPs and the LHC*. JHEP, 11:108, 2015.

List of Acronyms

A

ATLAS	Almost Toroidal LHC ApparatuS

B

BU	Builder Unit

C

CERN	European Organization for Nuclear Research
CHS	charged hadron subtraction
CMB	Cosmic Microwave Background
CMS	Compact Muon Solenoid
CSC	Cathode Strip Chambers

D

DAQ	data acquisition
DQM	Data Quality Monitoring
DT	Drift Tubes

E

ECAL	electromagnetic calorimeter

F

FED	Front End Driver
FSR	final state radiation
FU	Filter Unit

G

GSF	Gaussian-sum filter

H

HCAL	hadronic calorimeter
HLT	High-Level Trigger
HSCP	heavy stable neutral particle

I

IP	interaction point
ISR	initial state radiation

J

JER	jet energy resolution

L

L1	Level-1
LEIR	Low Energy Ion Ring
LEP	Large Electron Positron
LHC	Large Hadron Collider
LO	leading order

N

NLO	next-to-leading order

P

PDF	parton distribution function
PF	particle flow
PS	Proton Synchrotron
PSB	Proton Synchrotron Booster

Q

QCD	Quantum Chromodynamics

R

RF	radio-frequency
ROC	read-out chip
RPC	Resistive Plate Chambers
RU	Readout Unit

S

SIDM	self-interacting dark matter
SIMP	strongly interacting massive particle
SPS	Super Proton Synchrotron
SUSY	supersymmetry

T

TEC	Tracker EndCaps
TIB	Tracker Inner Barrel
TID	Tracker Inner Disks
TOB	Tracker Outer Barrel

W

WIMP	weakly interacting massive particle